J9.4 TOWARD IMPROVED LAND SURFACE INITIALIZATION IN SUPPORT OF REGIONAL WRF FORECASTS AT THE KENYA METEOROLOGICAL SERVICE (KMS)

Jonathan L. Case*[1], John Mungai[2], Vincent Sakwa[2], Eric Kabuchanga[3], Bradley T. Zavodsky[4], and Ashutosh S. Limaye[5]

[1]*ENSCO, Inc./Short-term Prediction Research and Transition (SPoRT) Center, Huntsville, AL*
[2]*Kenya Meteorological Service, Nairobi, Kenya*
[3]*Regional Centre for Mapping of Resources for Development/NASA SERVIR-Africa*
[4]*NASA Marshall Space Flight Center/SPoRT Center*
[5]*NASA Marshall Space Flight Center/SERVIR*

1. INTRODUCTION

Flooding and drought are two key forecasting challenges for the Kenya Meteorological Service (KMS). Atmospheric processes leading to excessive precipitation and/or prolonged drought can be quite sensitive to the state of the land surface, which interacts with the planetary boundary layer (PBL) of the atmosphere providing a source of heat and moisture. The development and evolution of precipitation systems are affected by heat and moisture fluxes from the land surface, particularly within weakly-sheared environments such as in the tropics and sub-tropics. These heat and moisture fluxes during the day can be strongly influenced by land cover, vegetation, and soil moisture content. Therefore, it is important to represent the land surface state as accurately as possible in land surface and numerical weather prediction (NWP) models.

Enhanced regional modeling capabilities have the potential to improve forecast guidance in support of daily operations and high-impact weather over eastern Africa. KMS currently runs a configuration of the Weather Research and Forecasting (WRF) NWP model in real time to support its daily forecasting operations, making use of the NOAA/National Weather Service (NWS) Science and Training Resource Center's Environmental Modeling System (EMS) to manage and produce the KMS-WRF runs on a regional grid over eastern Africa.

Two organizations at the NASA Marshall Space Flight Center in Huntsville, AL, SERVIR and the Short-term Prediction Research and Transition (SPoRT) Center, have established a working partnership with KMS for enhancing its regional modeling capabilities through new datasets and tools. To accomplish this goal, SPoRT and SERVIR is providing enhanced, experimental land surface initialization datasets and model verification capabilities to KMS as part of this collaboration. To produce a land-surface initialization more consistent with the resolution of the KMS-WRF runs, the NASA Land Information System (LIS) is run at a comparable resolution to provide real-time, daily soil initialization data in place of data interpolated from the National Centers for Environmental Prediction (NCEP) Global Forecast System (GFS) model soil moisture and temperature fields. Additionally, real-time green vegetation fraction (GVF) data from the Visible Infrared Imaging Radiometer Suite (VIIRS) on the Suomi National Polar-orbiting Partnership (Suomi-NPP) satellite will be incorporated into the KMS-WRF runs, once it becomes publicly available from the National Environmental Satellite Data and Information Service (NESDIS). Finally, model verification capabilities will be transitioned to KMS using the Model Evaluation Tools (MET; Brown et al. 2009) package in conjunction with a dynamic scripting package developed by SPoRT (Zavodsky et al. 2014), to help quantify possible improvements in simulated temperature, moisture and precipitation resulting from the experimental land surface initialization. Furthermore, the transition of these MET tools will enable KMS to monitor model forecast accuracy in near real time.

This paper presents preliminary efforts to improve land surface model initialization over eastern Africa in support of operations at KMS. The remainder of this extended abstract is organized as follows: The collaborating organizations involved in the project are described in Section 2; background information on LIS and the configuration for eastern Africa is presented in Section 3; the WRF configuration used in this modeling experiment is described in Section 4; sample experimental WRF output with and without LIS initialization data are given in Section 5; a summary is given in Section 6 followed by acknowledgements and references.

2. COLLABORATING ORGANIZATIONS

The KMS, SERVIR, the Regional Centre for Mapping of Resources for Development (RCMRD), and the SPoRT Center have teamed together to provide enhanced modeling and verification capabilities to operations conducted at KMS. The collaboration being fostered in this modeling project is enabled through the strengths of each organization as described below.

2.1 Kenya Meteorological Service (KMS)

The KMS has a wide range of weather and climatological responsibilities over eastern Africa and the western Indian Ocean. Among these include providing meteorological and climatological services to agriculture, water resources management, military/civil aviation, private sector, and public

**Corresponding author address:* Jonathan Case, ENSCO, Inc., 320 Sparkman Dr., Room 3008, Huntsville, AL, 35805. Email: Jonathan.Case-1@nasa.gov

utilities for better utilizing natural resources for national development. KMS provides meteorological services and issues cyclone warnings for the western Indian Ocean to ensure safe shipping operations. They also administer surface and upper-air observations and maintain telecommunications for a timely collection and dissemination of meteorological data. Additionally, KMS conducts applied research activities and develops suitable meteorological training programs that are relevant to Kenya and other participating countries.

The KMS runs its own in-house configuration of the WRF EMS framework. These forecasts are currently generated in real-time on a domain with 7-km grid spacing that covers a significant portion of eastern Africa and adjacent parts of the western Indian Ocean. All initial and boundary conditions for the daily simulations are provided by the GFS model. A sample 60-h forecast of mean sea level pressure and 10-m winds from the model run initialized on 0000 UTC 24 February 2014 highlights the domain coverage of the current KMS-WRF (Figure 1).

2.2 NASA SERVIR project

SERVIR is a NASA-USAID joint project that seeks to "connect space to village" by enabling the use of Earth observations and research satellite datasets in developmental decision making throughout various international "hubs". SERVIR first began in the Central America and Caribbean region (i.e., "Mesoamerica") by establishing a regional service that provides a suite of analysis and visualization tools that integrate satellite and other geospatial data to support environmental monitoring and informed decision-making. The program focuses on national priorities and regional needs to harness the full potential of remote sensing and geospatial technologies. SERVIR focuses on developing applications and tools to cater to those needs along the societal benefits areas and themes identified by Group on Earth Observations.

The SERVIR project has since expanded to additional hubs in the Africa and Himalaya regions. In 2008, NASA partnered with RCMRD based in Nairobi, Kenya, and together they began setting up SERVIR's Africa hub. The SERVIR-Africa project builds upon the existing strengths of RCMRD and augments the data management and training capability at RCMRD. Efforts complement RCMRD's core mission and provide a springboard for the development of applications customized for the 19 member states of RCMRD. SERVIR-Himalaya began in 2010 at the International Centre for Integrated Mountain Development, with the overarching purpose to improve environmental decision-making in the Hindu Kush-Himalayan region through dissemination and analyses of earth observation information.

2.3 Regional Centre for Mapping of Resources for Development(RCMRD)

The RCMRD was established in Nairobi, Kenya in 1975 under the auspices of the United Nations Economic Commission for Africa and the then Organization of African Unity, known today as the African Union. RCMRD is an inter-governmental organization and currently has 19 Contracting Member States in the Eastern and Southern Africa Regions: Botswana, Burundi, Comoros, Ethiopia, Kenya, Lesotho, Malawi, Mauritius, Namibia, Rwanda, Seychelles, Somali, South Africa, South Sudan, Sudan, Swaziland, Tanzania, Uganda, and Zambia. The mission of RCMRD is to promote sustainable development through generation, application and dissemination of Geo-Information and allied Information and Communication Technology services and products in the Member States and beyond.

2.4 NASA SPoRT Center

The NASA SPoRT Center (Jedlovec 2013; Ralph et al. 2013; Merceret et al. 2013) focuses on transitioning unique NASA and NOAA observations and research capabilities to the operational weather community to improve short-term weather forecasts on a regional and local scale. SPoRT demonstrates the capability of NASA and NOAA experimental products to weather applications and societal benefit, and prepares forecasters for use of data for the next generation of operational satellites. SPoRT maintains a close collaboration with numerous NOAA/NWS weather forecast offices across the United States. Beginning in 2002 with NASA funds, SPoRT delivered its first NASA satellite-based products to the NOAA/NWS Advanced Weather Interactive Processing System in 2003. Since 2009, it has been co-funded by NOAA through satellite proving ground activities such as GOES-R and JPSS.

The successful paradigm of SPoRT is one that involves the forecaster/end-user at all levels of transition activities, as illustrated in Figure 2. A forecast challenge is first matched to a data product and a prospective solution is developed and demonstrated in a test bed environment within the end-user's decision support system. An appropriate product training is then developed followed by an assessment of the perceived product impact on forecast operations. If the product is not yet deemed mature enough for a full transition, then the cycle is repeated to improve the components of the product needing further development. Another important aspect of this process is to have a local end-user advocate who can promote assessment of the product in the operational test bed. It is through this transition-to-operations paradigm that SPoRT is teaming up with the SERVIR project, RCMRD (SERVIR-Africa), and KMS to provide additional tools and datasets (i.e., MET verification, LIS and VIIRS GVF) that have the potential to enhance operations at KMS.

3. NASA LIS AND AFRICA-LIS CONFIGURATION

3.1 LIS framework

The NASA LIS is a high performance land surface modeling and data assimilation system that integrates satellite-derived datasets, ground-based observations and model reanalyses to force a variety of LSMs (Kumar et al. 2006; Peters-Lidard et al. 2007). By using scalable, high-performance computing and data management technologies, LIS can run LSMs offline globally with a grid spacing as fine as 1 km to characterize land surface states and fluxes. LIS has also

been coupled to the Advanced Research WRF dynamical core (Kumar et al. 2007) for applications using the NASA Unified-WRF modeling framework.

3.2 East Africa-LIS Configuration

In the Africa-LIS configuration, version 3.2 of the Noah LSM (Ek et al. 2003; Chen and Dudhia 2001) is run in analysis mode (i.e., uncoupled from an NWP model) over much of east-central Africa at 0.03-degree grid spacing for a continuous long simulation. The soil temperature and volumetric soil moisture fields were initialized at constant values of 290 K and 20 % in all four Noah soil layers (0-10, 10-40, 40-100, and 100-200 cm) on 1 January 2011, followed by a sufficiently long integration using a 30-minute timestep to near real-time, in order to remove memory of the initial soil conditions. Three different LIS spin-up simulations were conducted and inter-compared using separate precipitation input data, as described in Section 3.2.2.

3.2.1 **Static input fields**

The Africa-LIS uses the International Geosphere-Biosphere Programme (IGBP) land-use classification (Loveland et al. 2000) as applied to the Moderate Resolution Imaging Spectroradiometer (MODIS) instrument (Friedl et al. 2010). All static and dynamic land surface fields are masked based on the IGBP/MODIS land-use classes. The soil properties are represented by the State Soil Geographic (STATSGO; Miller and White 1998) database – the same as used in the community WRF model.

Additional parameters include a 0.05° resolution maximum snow surface albedo derived from MODIS (Barlage et al. 2005) and a deep soil temperature climatology (serving as a lower boundary condition for the soil layers) at 3 meters below ground, derived from 6 years of Global Data Assimilation System (GDAS) 3-hourly averaged 2-m air temperatures using the method described in Chen and Dudhia (2001). GVF is represented by the same monthly climatology dataset (Gutman and Ignatov 1998) as used in the community WRF. However, future Africa-LIS configurations shall make use of the daily real-time global NESDIS VIIRS GVF product (Vargas et al. 2013), once it becomes publicly available.

3.2.2 **Multi-year LIS spin-ups**

The Noah LSM in all three Africa-LIS runs was initialized at 0000 UTC 1 January 2011, over a sufficiently large region to encompass the entire WRF EMS experimental simulation domain, as described in the upcoming Section 4. The simulations were run for over two years prior to use for real-time applications in order to remove memory of the unrealistic uniform soil initial conditions. The atmospheric forcing variables required to drive the LIS-Noah integration consist of surface pressure, 2-m temperature and specific humidity, 10-m winds, downward-directed shortwave and longwave radiation, and precipitation rate. In the long-term simulation, all atmospheric forcing variables are provided by 3-hourly GDAS 0–9-h analyses and short-term forecast files (Parrish and Derber 1992; NCEP EMC 2004). Input precipitation forcing in the three spin-up simulations were given by (1) GDAS modeled 3-hourly precipitation rates, (2) three-hour precipitation from the version 7 Tropical Rain Measurement Mission (TRMM) 0.25-deg multi-satellite product (Ostrenga et al. 2013), and (3) half-hourly precipitation from the NCEP Climate Prediction Center Morphing (CMORPH) technique 8-km product (Joyce et al. 2004). The Noah LSM solution ultimately converges to a modeled state based on the GDAS and GDAS/TRMM/CMORPH precipitation input.

An inter-comparison of LIS-Noah runs was made with the three precipitation forcing inputs to examine the level of detail and reasonableness of the resulting soil moisture distribution. No formal validation was performed; however, the GDAS-exclusive spin-up run exhibited unrealistic patterns of alternating moist and dry soil moisture at coarse resolution, not consistent with the complex topography present across a good portion of east-central Africa.

A comparison of 30-day accumulated precipitation from the three different sources is given in Figure 3 for a sample month early in the LIS spin-up simulations. As already suggested, the GDAS modeled 3-h precipitation rates accumulated over the 30 days ending 1 May 2011 (panel a) look highly "bubbly" and unrealistic. This pattern in the GDAS accumulated precipitation most likely arises from the relatively coarse resolution of the GDAS/GFS modeling system and its inability to resolve precipitation variations around complex terrain such as that found in east-central Africa. Meanwhile, the satellite-derived precipitation rates from 3-h TRMM (panel b) and 0.5-h CMORPH (panel c) exhibit more realistic structure, and have similar large-scale patterns of maxima and minima relative to one another. The similar patterns of 30-day accumulated precipitation between TRMM and CMORPH were seen throughout the multi-year LIS spin-up (not shown), instilling more confidence in the reliability of these independent products for driving the land surface model integration. Ultimately, we chose the CMORPH precipitation product to drive the real-time Africa-LIS due to its higher spatial resolution and temporal frequency.

3.2.3 **Real-time LIS restarts for initializing WRF**

The real-time Africa-LIS cycle is initiated twice daily at 0215 and 1415 UTC from history re-start files of the simulation using GDAS-CMORPH forcing. The LIS restart times are determined primarily on the time-availability of GDAS 0–9-h files. The GDAS analyses and short-term forecasts have ~6–7-h delay following the GDAS/GFS 6-hourly cycle. For example, the previous day's 1800 UTC GDAS cycle files are available by ~0100 UTC, and are thus used to drive the 0215 UTC Africa-LIS integration through 0300 UTC. The CMORPH file production is done on a daily basis, with the previous day's files available by ~2100 UTC. The Africa-LIS cycle is completed in time for the real-time WRF-EMS runs, as described below.

4. CONTROL & EXPERIMENT WRF EMS SETUP

To begin examining the impacts of alternative land surface initialization over eastern Africa, the WRF EMS was configured to run a "Control" and "Experiment" configuration on a domain similar to the current real-

time 7-km KMS simulations. For the experiment at hand, a nested grid configuration approach was taken such that the inner nested grid covers approximately the same geographical area as the KMS 7-km runs. The model domain consists of an outer domain over north-eastern Africa with 12-km horizontal grid spacing, and an inner nested domain at 4-km grid spacing, as depicted in Figure 4. A single WRF EMS forecast is conducted daily, each for the Control and Experiment runs. Both simulations are initialized at 0000 UTC, and run out to 48 hours, with the Experiment run executing first at 0405 UTC each day, followed by the Control run executing at 0945 UTC daily. Using an option available in the EMS, concurrent post-processing is conducted during model execution such that graphics from the hourly model output are posted to an internal web page in an expedient manner each day.

The additional configuration detail worth noting is the contrast between the Control and Experiment setup. In the Control, the NCEP GFS model 3-hourly forecasts provide all initial and boundary conditions to each daily WRF run. Meanwhile, in the Experiment runs, the GFS model land surface initialization fields (consisting of soil moisture, soil temperature, skin temperature, and snow water equivalent) are replaced by the higher-resolution Africa-LIS fields at the valid 0000 UTC initialization hour. Other specific details on the model domain, timestep, and choice of physical parameterization schemes are summarized in Table 1.

5. SAMPLE EXPERIMENTAL WRF OUTPUT

This section provides a brief sample of preliminary output differences between Control and Experiment WRF EMS runs for a heavy rainfall case from 12-13 December 2013. KMS indicated that a few rain gauge stations in central and coastal Kenya experienced 24-hour rainfall in excess of 50 mm, especially for the period from 0600 UTC 12 December to 0600 UTC 13 December. The CMORPH satellite estimated rainfall during the 24-h period ending 0600 UTC 13 December (Figure 5) shows pockets of very heavy rainfall in southern and western Kenya and especially in Tanzania through Uganda and eastern Congo. Select model differences are shown to provide a flavor for the type of impacts seen by the Africa-LIS initialization.

5.1 LIS Versus GFS LSM Initialization

The difference in the top-layer volumetric soil moisture initialization (0-10 cm) is presented in Figure 6. The figure illustrates the marked difference in the level of detail between the GFS 0.5-degree initialization data (panels a and c) and the Africa-LIS 0.03-degree initialization data (panels b and d). Soil moisture patterns are more clearly defined in the LIS initialization within the complex terrain and individual large mountains, even on the 12-km Domain 1 (panels a and b). The Africa-LIS generally provides a drier solution over Kenya, Tanzania, Uganda, Rwanda, and Burundi, but has slightly more widespread wetness over eastern Congo. The top soil layer responds most rapidly to incoming precipitation, and interacts directly with the lower atmosphere in areas of bare soil.

5.2 Control Versus Experiment WRF

The different land surface initialization typically impacts the evolution of low-level temperature, dew point temperature, and the height of the PBL, all of which affect the distribution of surface-based Convective Available Potential Energy (CAPE). Areas of more moist (drier) soils should see a corresponding decrease (increase) in 2-m temperature (dew point temperature), decrease (increase) in the height of the PBL, and overall increase (decrease) in moist static energy per unit mass, typically manifested in the CAPE calculation. This land surface feedback mechanism has been explained in detail by Eltahir (1998) and Findell and Eltahir (2003).

The surface-based CAPE for the 12-h WRF forecast is given in Figure 7. Both simulations show the highest CAPE areas over Tanzania and Uganda, along with an axis of maximum CAPE extending through central Kenya. The CAPE maximum over central Kenya in the Experiment run, however, is somewhat diminished, consistent with the drier LIS soil moisture initialization in this corridor (Figure 6).

The WRF forecast 24-h precipitation on Domain 2, ending at 0600 UTC 13 December (Figure 8) shows a general over-prediction of the coverage of higher-intensity precipitation (> 20 mm given by the dark blue shading) when compared to the CMORPH estimated precipitation in Figure 5, especially over south-western Kenya. Both simulations suggest the potential for maximum rainfall totals to exceed 200 mm in isolated areas of southern Kenya and northern Tanzania, which is likely an over-prediction of intensity.

5.3 Sample WRF Model Verification Differences

Using the capabilities of MET and the SPoRT dynamic "wrapper" scripts, numerous verification plots were generated to compare the skill of each daily Control and Experiment WRF EMS simulation. Sample output verification graphs are shown in Figure 9 comparing the 0000 UTC 12 December 2013 Control and Experiment simulations. The observation locations used in the point verification for surface and upper-air variables are plotted using the IDL visualization software by querying the contents of the MET output statistics files (panel a). This plot shows that most observations are surface-based and located in the central and southwestern portion of Domain 2 (inner box of panel a) and in the northern portion of Domain 1. The observations found within the NCEP GDAS assimilation prepbufr files were used for generating verification statistics by running the "pb2nc" (prepbufr to netcdf) utility found in the MET software package. It should be noted, however, that data from virtually any point observations network can be used for verification in MET by reformatting the data into simple ascii columns and running the MET utility ascii2nc (ascii to netcdf) to prepare netcdf observation files, according to the instructions for the ascii2nc program within the MET User's Guide.

A comparison of the mean errors for 2-m temperature (Figure 9b) and 2-m dew point temperature (Figure 9c) on Domain 1 further supports the feedback mechanism described above in Section

5.2. The generally drier LIS soil moisture initialization compared to the GFS model resulted in systematically higher forecast 2-m temperature and lower 2-m dew point temperature, as seen in the mean error/bias plot in panels b and c, especially from the 6-h forecast and beyond. In the case of 2-m temperature, the inclusion of LIS land surface initialization slightly improved the prevailing cool bias in 2-m temperature, whereas it slightly degraded a small dry bias in 2-m dew point temperature for most forecast hours. The net result is rather mixed, as is often the case with NWP model sensitivity studies, thus evaluations over longer time periods and numerous case studies are typically required to formulate more robust conclusions.

The Heidke Skill Score (HSS) for 24-h accumulated precipitation is given in Figure 9d, which shows slightly higher skill in the LIS-initialized runs beginning around forecast hour 34. The HSS is often a preferred measure for assessing forecast precipitation skill (as opposed to the traditional threat score, or Critical Success Index) since the HSS accounts for random chance in its formulation. Although not shown here in the plots, the statistical significance of MET output statistics can be easily determined between different model runs because the MET software outputs the confidence intervals of each statistic as a function of forecast hour. The confidence intervals are defined by the user in the MET input files (e.g., 95th percentile). Statistical significance is achieved if the range from the lower to upper confidence intervals of model result 1 is outside of the confidence interval range of model result 2.

5.4 Preview of VIIRS GVF in LIS and WRF

The SPoRT Center was provided sample files of the NESDIS VIIRS GVF global product from early August 2013. These sample files were used to develop the capability to ingest the daily VIIRS GVF into both the LIS and WRF EMS frameworks, thereby accelerating the assessment and transition of the VIIRS GVF product into experimental operations, once the data become publicly available in near real-time. SPoRT completed the coding required to ingest these data into LIS and WRF. However, since the NESDIS VIIRS GVF product is still undergoing validation (Vargas, personal communication), these data should not be considered of final science-quality. Nevertheless, the VIIRS GVF data show promise in the applications to NWP and land surface modeling.

Figure 10 shows a comparison between the monthly climatology GVF time-interpolated to 23 August, and a daily VIIRS GVF composite valid on 7 August 2013, interpolated to both nested WRF grids. Despite the slight time displacement between 23 August and the 7 August 2013 valid day of the real-time VIIRS GVF, good agreement is seen among the large-scale patterns of GVF maxima and minima across the modeling domains. Maximum GVF in both datasets occurs from southwestern Kenya and western Ethiopia, westward to northern Congo and southern Sudan. Another strip of maximum GVF is seen along the Indian Ocean coast from southern Somalia to eastern Tanzania, although GVF values are considerably higher in the VIIRS product. Minimum values of GVF extend from northern Tanzania to eastern Kenya, eastern Ethiopia, and much of Somalia. What is clearly noticeable in the VIIRS GVF product is the markedly higher amount of detail due to the differences in resolution between the coarse climatology product (~0.144-deg) and the VIIRS GVF data (4 km). The combination of higher product resolution on the order of local-regional NWP model grid spacing and real-time satellite input has the potential to greatly improve surface-atmosphere heat flux partitioning, particular during anomalies such as the early or late onset of wet seasons.

A comparison of the 48-h forecast surface-based CAPE reveals that generally minor differences occurred for this particularly simulation. Slightly higher CAPE can be found in the WRF simulation using VIIRS GVF over parts of inland Somalia and the northern Congo associated with higher VIIRS GVF (Figure 11 compared to Figure 10). Conversely, slightly lower CAPE is seen over eastern Sudan where the VIIRS GVF are lower. In general, higher GVF correlates with increased evapotranspiration, lower 2-m temperatures, higher 2-m dew points, and ultimately higher surface-based CAPE (Case et al. 2014). Additional simulation experiments are planned with Africa-LIS and WRF EMS runs incorporating the real-time daily VIIRS GVF after the data become available.

6. SUMMARY AND FUTURE DIRECTION

This paper presented the framework for a modeling experiment over eastern Africa in which an alternative land surface initialization is provided to regional WRF EMS model runs, through the use of offline LIS-Noah land surface simulations. This experiment was made possible through a collaboration between operational, and research-to-transition organizations which include the Kenya Meteorological Service, SERVIR, RCMRD, and SPoRT. Preliminary results suggest relatively minor impacts on real-time WRF EMS simulations, however, the sensitivity to land surface states may be most critical during transitions between dry and wet regimes (and vice versa). Additional analysis is required through composite verification statistics accumulated for longer time periods, as well as an examination of additional case studies, particularly those of high impact to end-users of KMS services.

Future work shall also include the incorporation of daily global VIIRS GVF data, which will be generated in near real-time by NOAA/NESDIS at a future date to be determined. To accelerate the experimental implementation of VIIRS GVF, SPoRT has already developed the code infrastructure to incorporate the data into both the LIS and WRF EMS frameworks. Once the data become available, SPoRT will re-run LIS in order to incorporate the VIIRS GVF into a new spin-up simulation. Real-time vegetation conditions should help improve the accuracy of LIS soil moisture estimates during the spin-up integration, since the VIIRS GVF will provide realistic vegetation anomalies that respond to weather and climate anomalies, as measured by the Suomi-NPP satellite. The output from the new LIS run with VIIRS GVF data will subsequently initialize WRF EMS runs that also incorporate real-time

VIIRS GVF data in place of the monthly climatology GVF.

Looking further ahead, the assimilation of satellite soil moisture estimates through the built-in Ensemble Kalman Filter algorithm (e.g., Kumar et al. 2008, 2009; Blankenship et al. 2014) may further enhance LIS soil moisture output for near real-time applications. Targeted data may include Europe's Soil Moisture Ocean Salinity and NASA's upcoming Soil Moisture Active-Passive missions.

ACKNOWLEDGEMENTS/DISCLAIMERS

This research was funded by Drs. Tsengdar Lee and Nancy Searby of the NASA Science Mission Directorate's Earth Science Division in support of the SPoRT and SERVIR projects, respectively. Mention of a copyrighted, trademarked or proprietary product, service, or document does not constitute endorsement thereof by the authors, ENSCO Inc., the Kenya Meteorological Service, SERVIR, the Regional Centre for Mapping of Resources for Development, the Short-term Prediction Research and Transition Center, the National Aeronautics and Space Administration, the United States government, or Kenya government. Any such mention is solely for the purpose of fully informing the reader of the resources used to conduct the work reported herein.

REFERENCES

Barlage, M., X. Zeng, H. Wei, and K. E. Mitchell, 2005: A global 0.05° maximum albedo dataset of snow-covered land based on MODIS observations. *Geophys. Res. Lett.,* **32,** L17405, doi:10.1029/2005GL022881.

Blankenship, C. B., J. L. Case, and B. T. Zavodsky, 2014: Assimilation of SMOS soil moisture retrievals in the Land Information System. Preprints, *28th Conf. on Hydrology,* Atlanta, GA, Amer. Meteor. Soc., P53. [Available online at https://ams.confex.com/ams/94Annual/webprogram/Paper233646.html]

Brown, B. G., J. H. Gotway, R. Bullock, E. Gilleland, T. Fowler, D. Ahijevych, and T. Jensen, 2009: The Model Evaluation Tools (MET): Community tools for forecast evaluation. Preprints, 25th Conf. on International Interactive Information and Processing Systems (IIPS) for Meteorology, Oceanography, and Hydrology, Phoenix, AZ, Amer. Meteor. Soc., 9A.6. [Available online at http://ams.confex.com/ams/pdfpapers/151349.pdf.]

Case, J. L., F. J. LaFontaine, J. R. Bell, G. J. Jedlovec, S. V. Kumar, and C. D. Peters-Lidard, 2014: A real-time MODIS vegetation product for land surface and numerical weather prediction models. *Trans. Geosci. Remote Sens.,* **52(3),** 1772-1786.

Chen, F., and J. Dudhia, 2001: Coupling an advanced land-surface/hydrology model with the Penn State/NCAR MM5 modeling system. Part I: Model description and implementation. *Mon. Wea. Rev.,* **129,** 569-585.

Ek, M. B., K. E. Mitchell, Y. Lin, E. Rogers, P. Grunmann, V. Koren, G. Gayno, and J. D. Tarpley, 2003: Implementation of Noah land surface model advances in the National Centers for Environmental Prediction operational mesoscale Eta model. *J. Geophys. Res.,* **108 (D22),** 8851, doi:10.1029/2002JD003296.

Eltahir, E. A., 1998: A soil moisture-rainfall feedback mechanism: 1. Theory and observations. *Water Resour. Res.,* **34,** 765-776.

Findell, K. L., and E. A. Eltahir, 2003: Atmospheric controls on soil moisture-boundary layer interactions. Part II: Feedbacks within the Continental United States. *J. Hydrometeor.,* **4,** 570-583.

Friedl, M. A., D. Sulla-Menashe, B. Tan, A. Schneider, N. Ramankutty, A. Sibley, and X. Huang, 2010: MODIS Collection 5 global land cover: Algorithm refinements and characterization of new datasets. *Remote Sens. Environ.,* **114,** 168-182.

Gutman, G. and A. Ignatov, 1998: Derivation of green vegetation fraction from NOAA/AVHRR for use in numerical weather prediction models. *Int. J. Remote Sensing,* **19,** 1533-1543.

Jedlovec, G., 2013: Transitioning Research Satellite Data to the Operational Weather Community: The SPoRT Paradigm. *Geoscience and Remote Sensing Newsletter*, March, L. Bruzzone, editor, Institute of Electrical and Electronics Engineers, Inc., New York, 62-66.

Joyce, R. J., J. E. Janowiak, P. A. Arkin, and P. Xie, 2004: CMORPH: A method that products global precipitation estimates from passive microwave and infrared data at high spatial and temporal resolution. *J. Hydrometeor.,* **5,** 487-503.

Kumar, S. V., and Coauthors, 2006. Land Information System – An Interoperable Framework for High Resolution Land Surface Modeling. *Environmental Modeling & Software,* **21 (10),** 1402-1415, doi:10.1016/j.envsoft.2005.07.004.

_____, C. D. Peters-Lidard, J. L. Eastman, and W.-K. Tao, 2007: An integrated high-resolution hydrometeorological modeling testbed using LIS and WRF. *Environmental Modeling & Software,* **23 (2),** 169-181, doi: 10.1016/j.envsoft.2007.05.012.

_____, R. H. Reichle, R. D. Koster, W. T. Crow, and C. D. Peters-Lidard, 2009: Role of subsurface physics in the assimilation of surface soil moisture observations. *J. Hydrometeor.,***10,** 1534-1547.

_____, _____, C. D. Peters-Lidard, R. D. Koster, X. Zhan, W. T. Crow, J. B. Eylander, and P. R. Houser, 2008: A land surface data assimilation framework using the Land Information System: Description and applications. *Adv. Water Res.,***31,** 1419-1432.

Loveland, T. R., B. C. Reed, J. F. Brown, D. O. Ohlen, Z. Zhu, L. Yang, and J. W. Merchant, 2000: Development of a global land cover characteristics database and IGBP DISCover from 1 km AVHRR data. *Int. J. Remote Sensing,* **21,** 1303-1330.

Merceret, F. J., T. P. O'Brien, W. P. Roeder, L. L. Huddleston, W. H. Bauman III, and G. J. Jedlovec, 2013: Transitioning research to operations: Transforming the "valley of death" into a "valley of opportunity". *Space Weather,* **11**, 1-4.

Miller, D. A. and R. A. White, 1998: A Conterminous United States multi-layer soil characteristics data set for regional climate and hydrology modeling. *Earth*

Interactions, 2. [Available on-line at http://EarthInteractions.org].

NCEP EMC, 2004: SSI Analysis System 2004. NOAA/NCEP/Environmental Modeling Center Office Note 443, 11 pp., April, 2004. [Available online at http://www.emc.ncep.noaa.gov/officenotes/newernotes/on443.pdf]

Ostrenga, D., Z. Liu, W. Teng, and S. J. Kempler, 2013: Newly released version 7 TRMM multi-satellite precipitation analysis (TMPA) products and data services at GES DISC. Preprints, *29th Conf. on Environmental Information Processing Technologies,* Austin, TX, Amer. Meteor. Soc., P13. [Available online at https://ams.confex.com/ams/93Annual/webprogram/Paper220338.html]

Parrish, D. F., and J. C. Derber, 1992: The National Meteorological Center's spectral statistical-interpolation analysis system. *Mon. Wea. Rev.,* **120,** 1747-1763.

Peters-Lidard, C. D., and Coauthors, 2007: High-performance Earth system modeling with NASA/GSFC's Land Information System. *Innovations Syst. Softw. Eng.,* **3,** 157-165.

Ralph, F. M., and Coauthors, 2013: The emergence of weather-related test beds linking research and forecasting operations. *Bull Amer. Meteor. Soc.,* **94,** 1187-1211.

Vargas, M., Z. Jiang, J. Ju, and I. A. Csiszar, 2013: EVI based green vegetation fraction derived from Suomi NPP-VIIRS. Preprints, *Ninth Symp. Future Operational Env. Sat. Systems,* Austin, TX, Amer. Meteor. Soc., P689.

Zavodsky, B. T., J. L. Case, J. H. Gotway, K. D. White, J. M. Medlin, L. Wood, and D. B. Radell, 2014: Development and implementation of dynamic scripts to support local model verification at National Weather Service Weather Forecast Offices. Preprints, 30th Conference on Environmental Information Processing Technologies, Atlanta, GA, Amer. Meteor. Soc., P500. [Available online at https://ams.confex.com/ams/94Annual/webprogram/Paper232418.html]

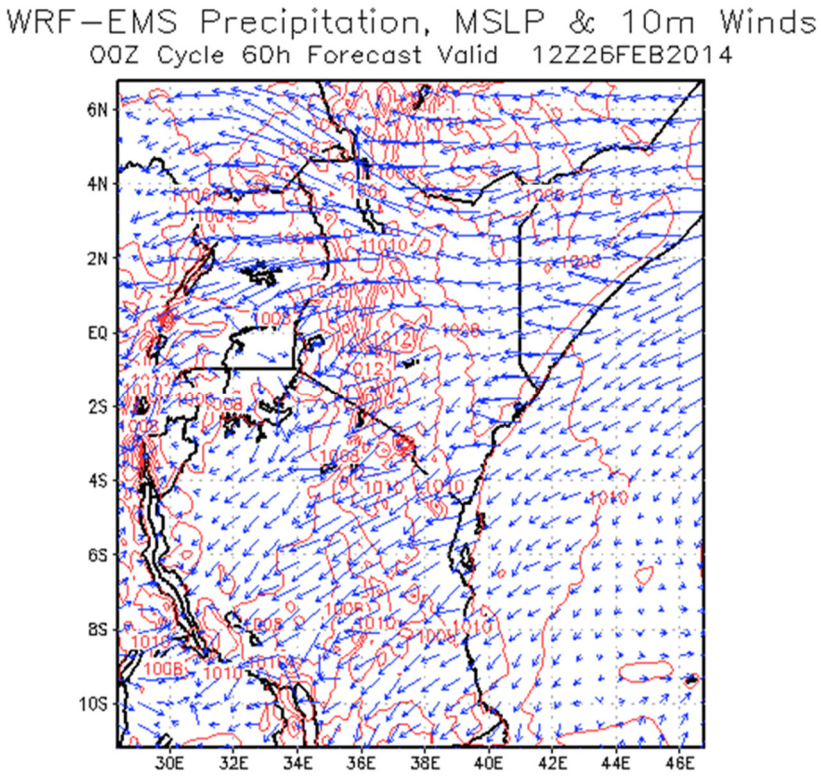

Figure 1. Sample 60-h forecast of mean sea level pressure and 10-m winds from the current operational 7-km KMS-WRF, for the run initialized at 0000 UTC 24 February 2014 and valid at 1200 UTC 26 February 2014.

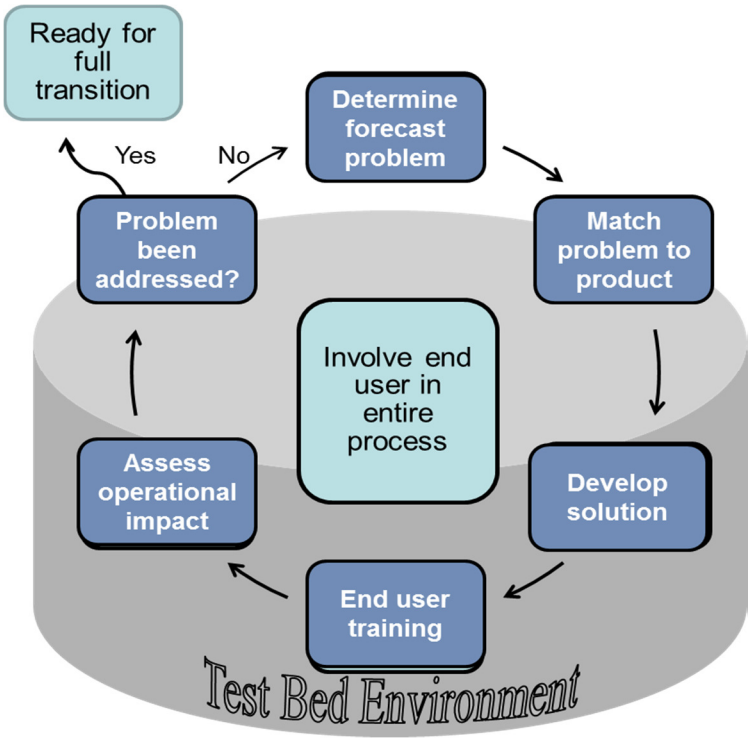

Figure 2. Illustration of the SPoRT paradigm of transitioning research to operations in a test bed environment.

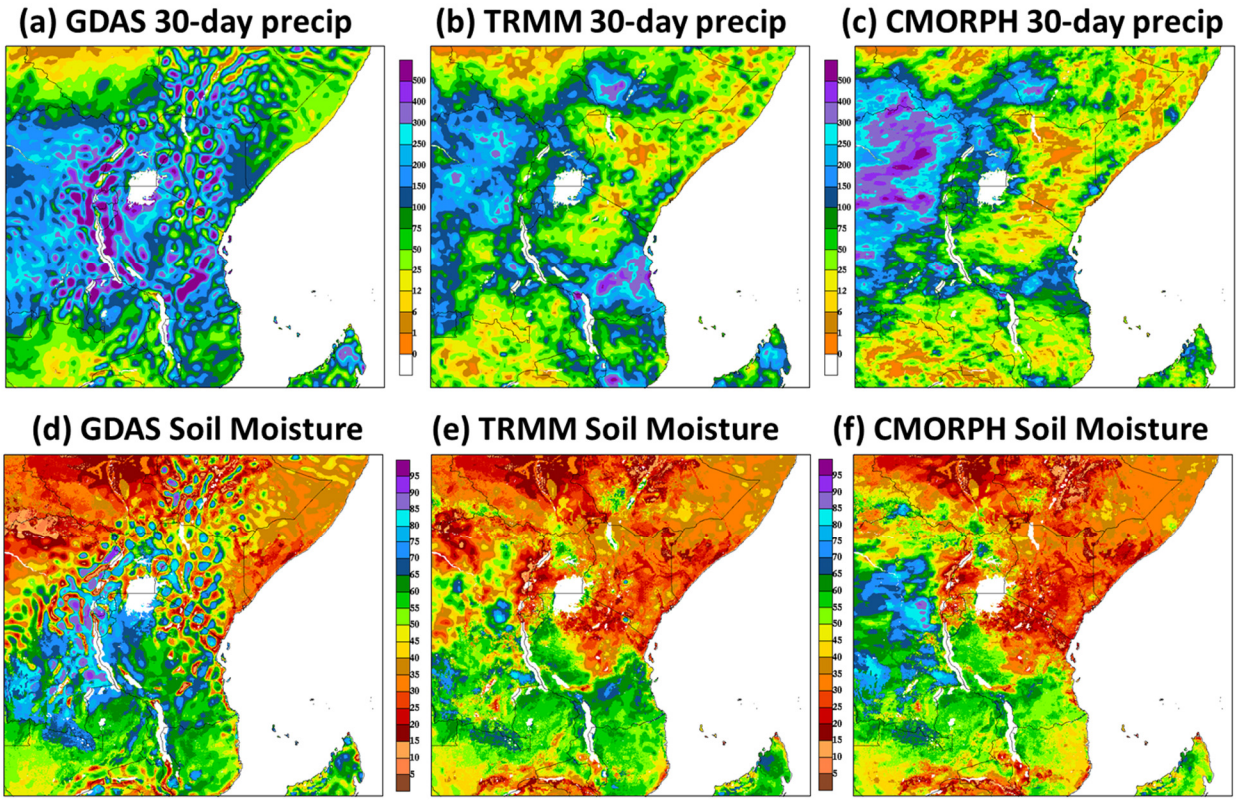

Figure 3. Inter-comparison of 30-day accumulated precipitation for (a) GDAS, (b) TRMM, and (c) CMORPH; and LIS-Noah column-integrated, 0-200 cm relative soil moisture for the simulation using precipitation from (d) GDAS, (e) TRMM, and (f) CMORPH. Each image is valid on 1 May 2011, after 5 months of LIS-Noah integration.

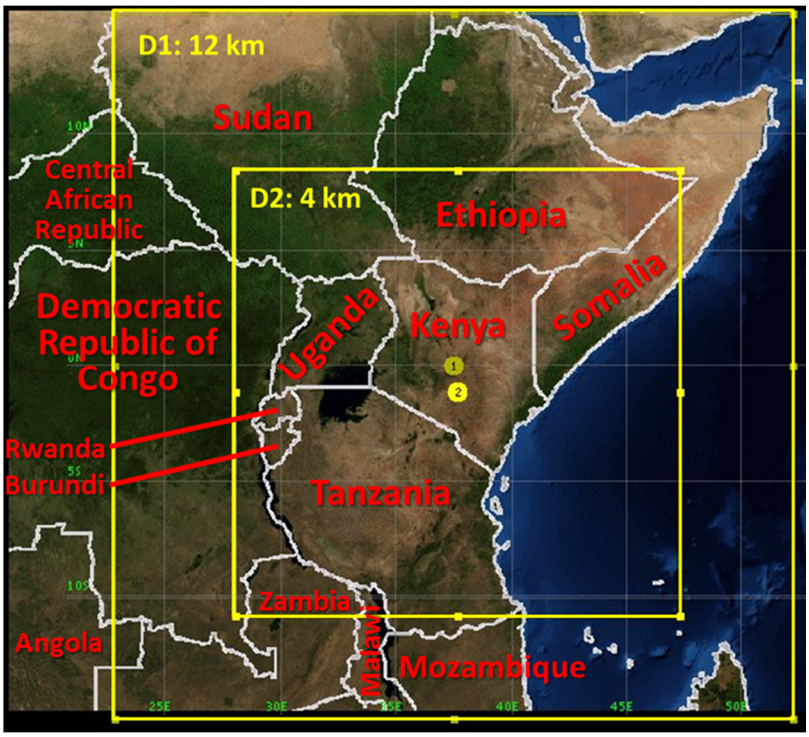

Figure 4. Depiction of the experimental WRF EMS domain configured over eastern Africa to compare the impacts of alternative land surface initialization datasets.

Table 1. Configuration details for the control and experiment WRF EMS runs over eastern Africa.

Configuration Detail	Specifications / selections
Model grid: Domain 1	271 x 281 with 12-km spacing
Model grid: Domain 2	532 x 532 with 4-km spacing; 1-way nesting
Vertical sigma levels	42 levels; pressure top of 30 mb
Domain 1 time step	72 seconds
Shortwave radiation parameterization	RRTM-G
Longwave radiation parameterization	RRTM-G
Convection parameterization	Kain-Fritsch (domain 1 only)
Microphysics scheme	Lin 5-class
Planetary boundary layer	Mellor-Yamada Nakanishi Niino (MYNN2)
Land surface model	Noah
Initialization and integration	0000 UTC, 48-h forecasts, once daily
Initial / Boundary conditions	NCEP GFS model 0-48-h forecasts in 3-h intervals
Sea surface temperature	NCEP Real-Time Global; fixed for simulation
Land surface initialization	Control: GFS 0-h soil temperature/moisture Experiment: LIS-Noah soil temperature/moisture

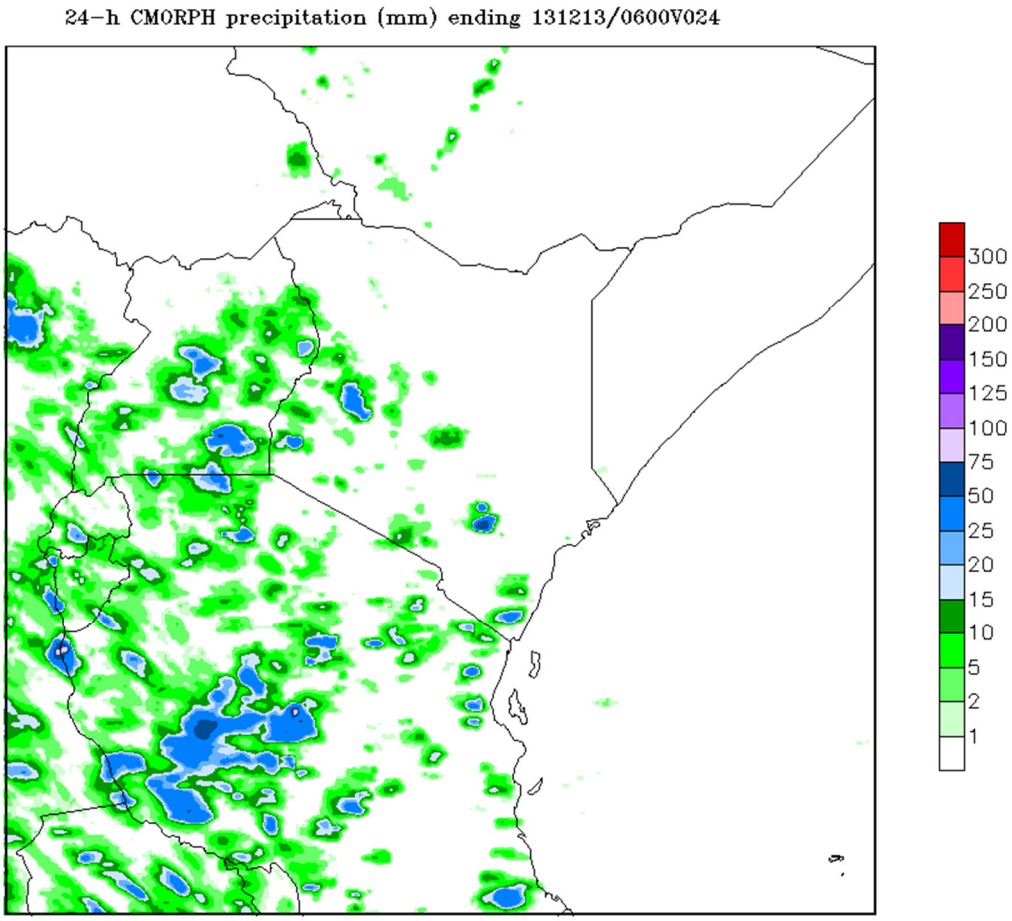

Figure 5. Estimation of accumulated precipitation by the CMORPH satellite-based product, for the 24-h period ending 0600 UTC 13 December 2013.

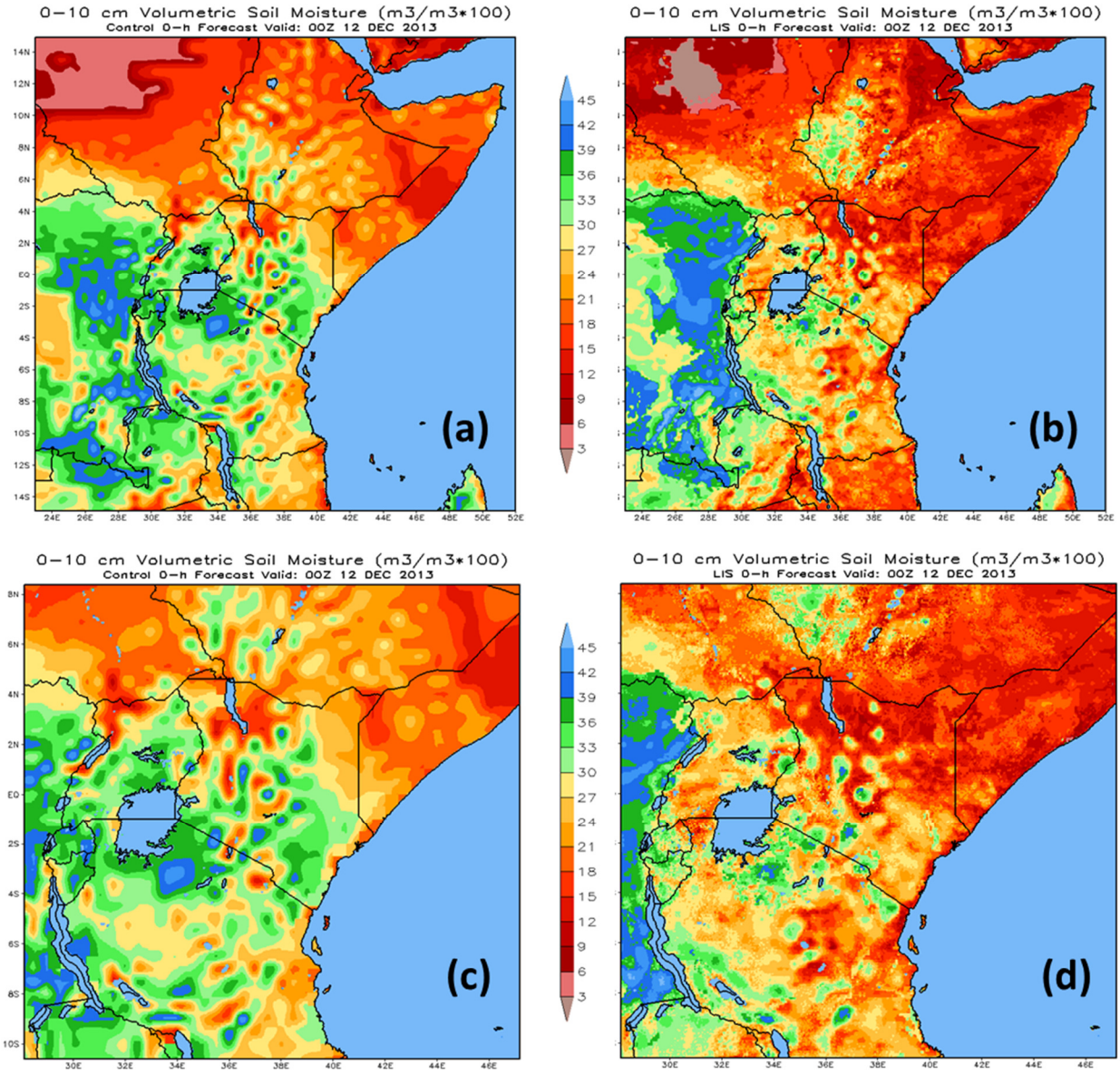

Figure 6. Comparison between 0-10 cm volumetric soil moisture initialization for a WRF EMS model run initialized at 0000 UTC 12 December 2013. Initial 0-10 cm soil moisture consists of (a) GFS 0-h field on Domain 1, (b) Africa-LIS on Domain 1, (c) GFS 0-h field on Domain 2, and (d) Africa-LIS on Domain 2.

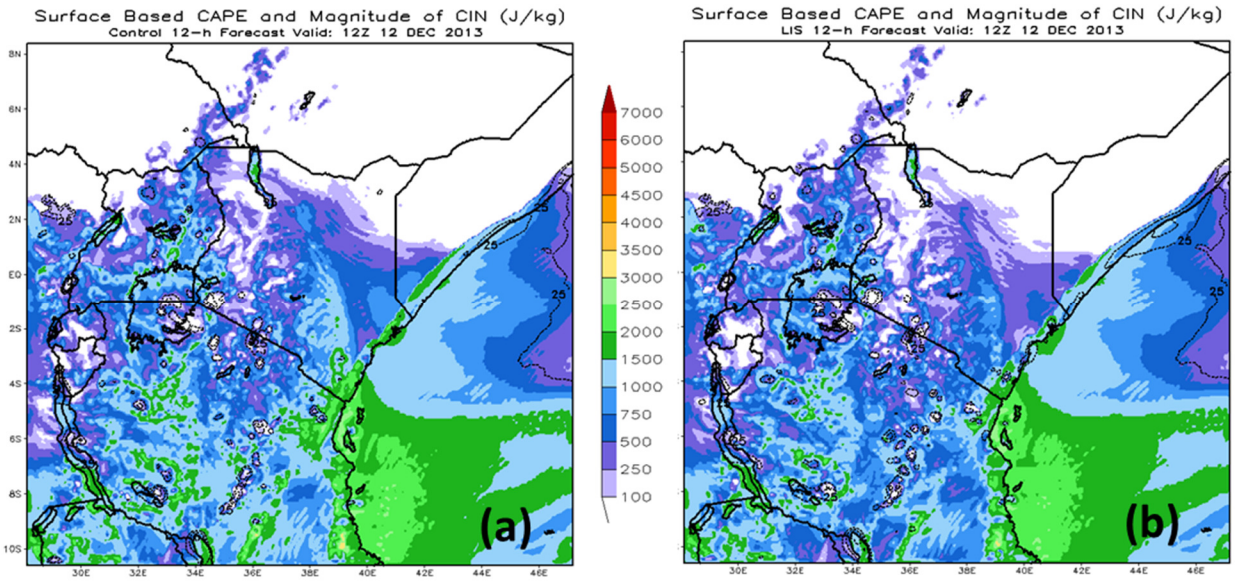

Figure 7. WRF EMS simulated surface-based Convective Available Potential Energy (CAPE) for the 12-h forecast valid 1200 UTC 12 December 2013. Images depicted are (a) Control WRF run with all GFS initialization data, and (b) Experiment WRF run with LIS land surface initialization data.

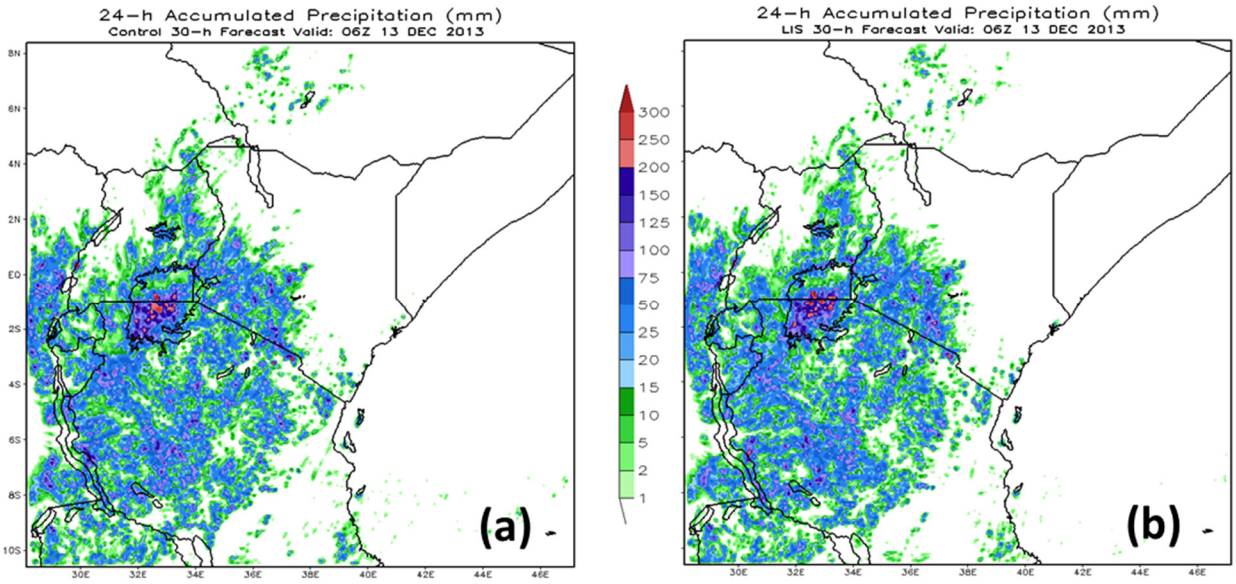

Figure 8. WRF EMS 24-h accumulated precipitation for period ending on the 30-h forecast valid at 0600 UTC 13 December 2013. Images depicted are (a) Control WRF run with all GFS initialization data, and (b) Experiment WRF run with LIS land surface initialization data.

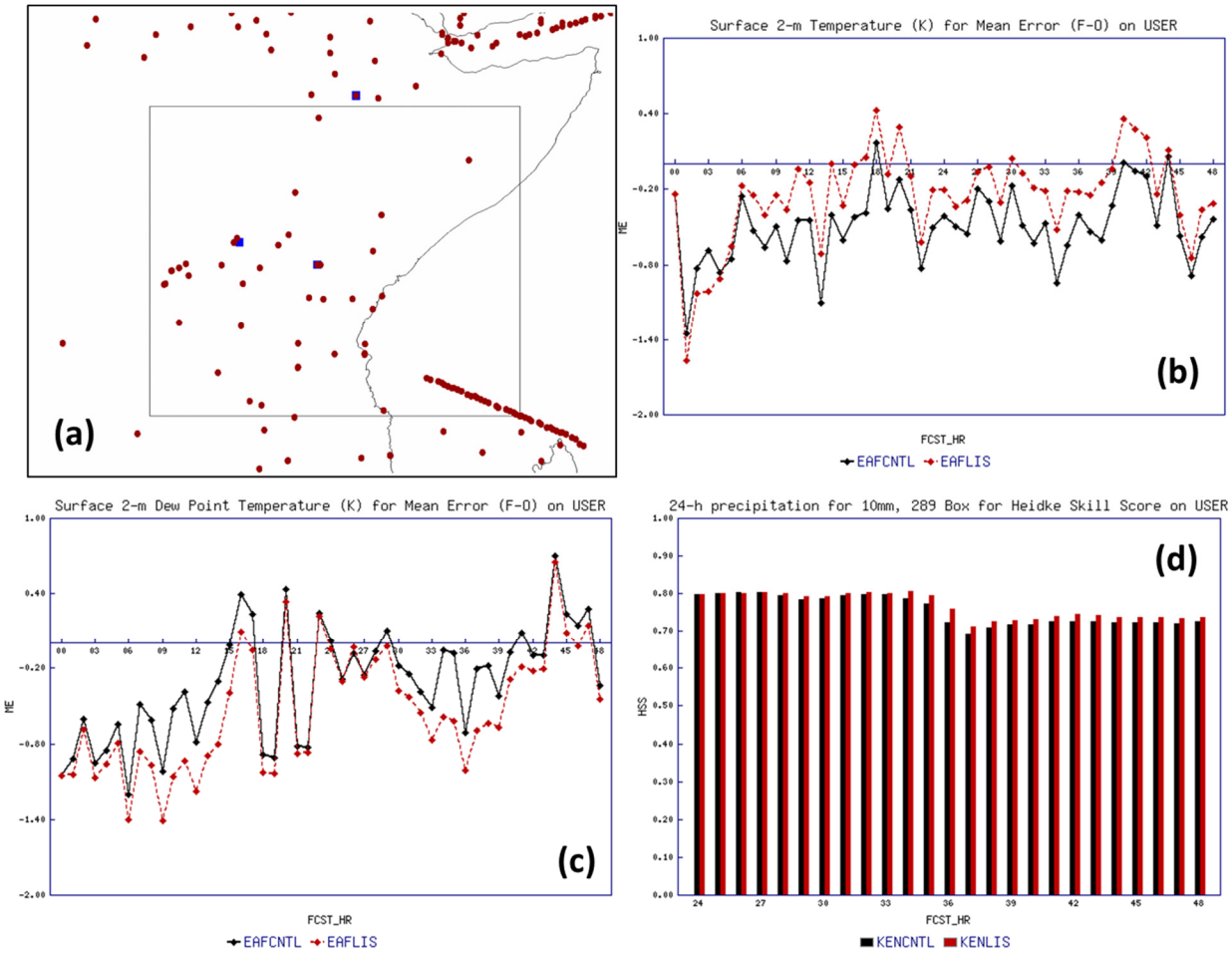

Figure 9. Sample verification output for the WRF EMS runs initialized at 0000 UTC 12 December 2013, using the SPoRT dynamic scripts running the MET verification package: (a) Distribution of surface (red dots) and upper-air (blue squares) observations in the GDAS prepbufr files used for point verification, and generated from MET output files using the IDL data visualization software, (b) Mean error (bias) of 2-m temperature forecasts on Domain 1, (c) Mean error of 2-m dew point temperature forecasts on Domain 1, and (d) Heidke Skill Score statistics for WRF forecast 24-h accumulated precipitation from the 24 to 48 hour forecasts on Domain 2. Red (black) lines/bars in panels b, c, and d indicate statistics for the Experimental (Control) WRF model runs.

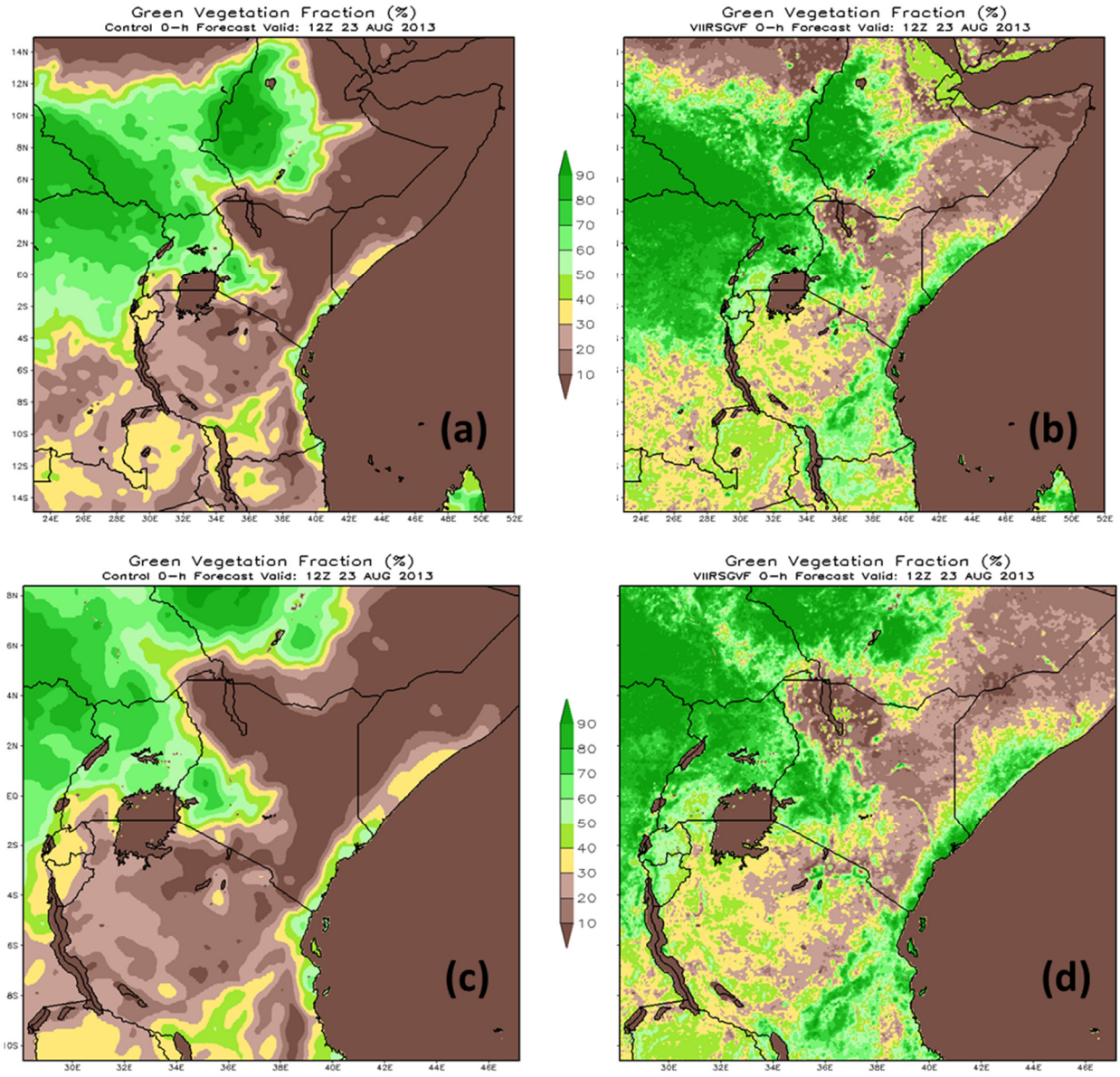

Figure 10. Comparison between input Green Vegetation Fraction (GVF) for a WRF EMS model run initialized at 1200 UTC 23 August 2013. Input GVF consists of (a) monthly climatology GVF on Domain 1, (b) sample NESDIS VIIRS GVF from 7 August 2013 interpolated to Domain 1, (c) monthly climatology GVF on Domain 2, and (d) NESDIS VIIRS GVF from 7 August 2013 interpolated to Domain 2.

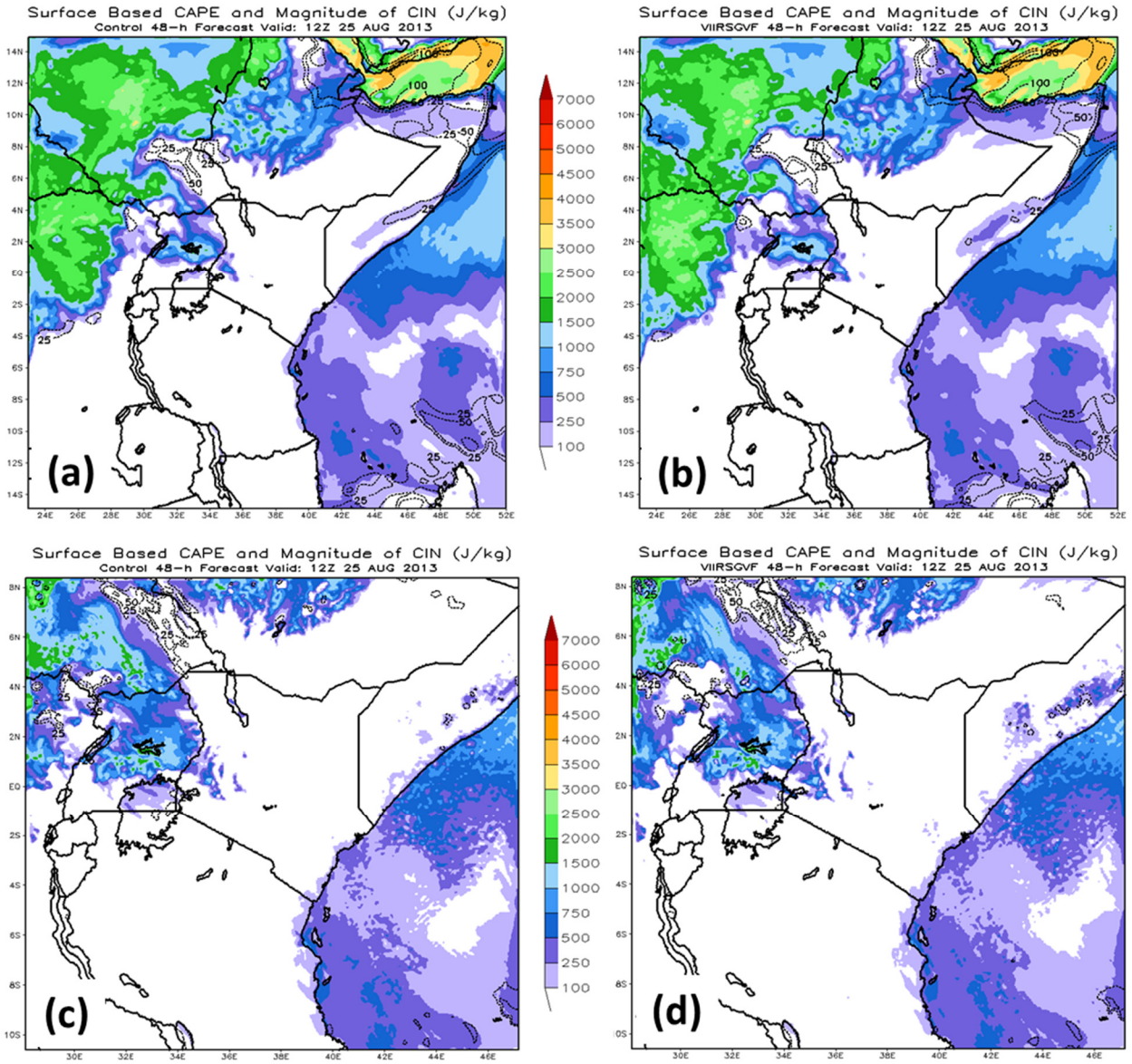

Figure 11. WRF EMS simulated surface based Convective Available Potential Energy (CAPE, J kg^{-1}) and Convective Inhibition (CIN, J kg^{-1}) for the 48-h forecast valid 1200 UTC 25 August 2013, comparing the (a) Control simulation on Domain 1, (b) WRF simulation with VIIRS GVF on Domain 1, (c) Control simulation on Domain 2, and (d) WRF simulation with VIIRS GVF on Domain 2.